Materials Science & Engineering A 605 (2014) 260–269

Contents lists available at ScienceDirect

Materials Science & Engineering A

journal homepage: www.elsevier.com/locate/msea

Effect of hot rolling reduction on microstructure, texture and ductility of strip-cast grain-oriented silicon steel with different solidification structures

Hong-Yu Song, Hai-Tao Liu*, Hui-Hu Lu, Hao-Ze Li, Wen-Qiang Liu, Xiao-Ming Zhang, Guo-Dong Wang

State Key Laboratory of Rolling and Automation, Northeastern University, Shenyang 110819, PR China

ARTICLE INFO

Article history:
Received 23 October 2013
Received in revised form
11 March 2014
Accepted 13 March 2014
Available online 20 March 2014

Keywords:
Strip casting
Grain-oriented silicon steel
Hot rolling reduction
Microstructure
Texture

ABSTRACT

Grain-oriented silicon steel as-cast strips with the average ferrite grain sizes of 161 μm and 367 μm were produced by twin-roll strip casting. Then the as-cast strips were reheated and hot rolled with different reductions of 5–50%. The microstructure and texture evolution were investigated by optical microscopy, X-ray diffraction, and electron backscattered diffraction methods. The elongations of the hot rolled strips were examined by the tensile tests and the fracture surfaces were observed by scanning electron microscope. It was found that the microstructure of both as-cast strips consisted of ferrite and martensite. The microstructure of all the hot rolled strips was composed of ferrite and pearlite and it was gradually refined with increasing hot rolling reduction in spite of different initial solidification structures. The hot rolled fine-grained strips showed much finer microstructure at the same hot rolling reduction and thus gave rise to higher elongations. A total reduction of more than 30% was required for the fine-grained strips to achieve relatively good ductility, while that for the coarse-grained strips was as high as 50%. With increasing hot rolling reduction, α and γ fibre textures were gradually enhanced at the expense of initial {001}⟨0vw⟩ fibre texture in all the hot rolled strips. Relatively strong Goss texture only evolved in the 50% hot rolled strips in spite of the different initial solidification structures, though the 50% hot rolled coarse-grained strip showed much stronger Goss texture.

1. Introduction

Grain-oriented silicon steel is an important soft magnetic material widely used as the core material in electrical transformers [1,2]. It is characterized by a sharp {110}⟨001⟩ preferred crystallographic orientation referred to as Goss texture [3]. Although the manufacturing process has been well developed since Goss first proposed the technological approach in 1934 [4], the conventional process is still complicated and interminable [5]. The recent progress in strip casting technology provides a possibility to produce grain-oriented silicon steel by a simpler processing than the conventional process [6,7] because strip casting can eliminate the thick slab casting and reduce hot rolling passes by supplying as-cast strips with thickness close to the conventional hot rolled sheets [8–11]. The strip casting steels are currently of considerable fundamental and technological interests worldwide by the researchers due to the superiorities of strip casting over the conventional processing. However, the researches on the strip-cast grain-oriented silicon steels have been rarely reported.

It is known that Goss texture originates in the hot rolling stage due to the shear deformation caused by high friction between the rolls and strip surfaces [12–15]. The inheritance of Goss texture has a significant influence on the nucleation of {110}⟨001⟩ secondary grains by way of structure memory [14] even after the cycle of normalization, cold rolling and subsequent annealing. In the conventional process, the thick slabs are continuously hot rolled in many passes with a total reduction exceeding 95%, and hence an amount of Goss orientation originates due to the severe shear deformation [14,15]. Besides, because of the heavy reduction the ductility of the hot rolled strips is greatly improved by refining the initial coarse solidification structure, which is suitable for the subsequent normalization and cold rolling. As for the strip casting process, thin strips are produced by direct casting from the steel melt with the high cooling rate of 10^2–10^4 K/s [16]. Liu et al. found that fully fine equiaxed and fully coarse columnar as-cast strips could be correspondingly obtained in ferritic steels by altering the superheat in the melt pool [17,18], and the former exhibited nearly random texture, while the latter showed strong {001} texture, which is significantly different from that of conventional hot rolled

* Corresponding author. Tel.: +86 24 83687220; fax: +86 24 23906472.
E-mail address: liuht@ral.neu.edu.cn (H.-T. Liu).

http://dx.doi.org/10.1016/j.msea.2014.03.052
0921-5093/

strip. Although the fine-grained or coarse-grained as-cast strips may suffer a little deformation during strip casting, the initial microstructure is composed of brittle solidification structure which is hard to be cold rolled. Therefore, it is essential to perform one or two passes hot-rolling after the strip casting so as to improve the ductility and modify the initial texture of the grain-oriented silicon steel as-cast strips. However, given that the thickness of the as-cast strip is close to that of the final hot rolled strip, the total hot rolling reduction is very limited and the effects of hot rolling reduction on microstructure, texture evolution and ductility have not been clarified. Furthermore, the effects of the initial solidification structure and texture on the microstructure, texture evolution and ductility of the hot rolled strips have also not yet been reported.

In the present work, the as-cast strips with different initial solidification structures and textures were produced by twin-roll strip casting and followed by hot rolling. The aim of this paper is to investigate the effects of the initial solidification structure, texture and hot rolling reduction on the microstructure, texture evolution and ductility of the hot rolled strips. This is an important part of the effort to produce the high-quality grain-oriented silicon steel by applying strip casting technology.

2. Experimental

Strip casting was carried out on a vertical type twin-roll caster, as described in detail earlier by Liu et al. [17–21]. The melt superheats in the pool were controlled to be 25 °C and 60 °C in order to produce the fine-grained and coarse-grained as-cast strips, respectively. The 3.1 mm thick as-cast strips were fabricated, yielding the following chemical composition (mass%): 2.9–3.2 Si, 0.16–0.20 Mn, 0.013–0.017 S, 0.055–0.060 C, 0.01–0.013 P, and Fe (balance). Both as-cast strips were reheated to 1150 °C and hot rolled with different rolling schedules in which some strips were hot rolled in one pass with a reduction of 5%, 20% and 30%, correspondingly, while the others in two passes with a total reduction of 50%. All the hot rolled strips were air-cooled to 550 °C, held for 90 min and then air-cooled to room temperature.

Metallographic specimens of the as-cast strips and hot rolled strips were machined, polished and etched with 4% nital. The microstructure along the longitudinal section (RD–ND) was observed by optical microscope (OM). The average ferrite grain size of the as-cast strips was measured using the line intercept method based on low magnification micrographs. The texture was quantitatively examined by measuring three incomplete pole figures {110}, {200} and {211} in the range of the polar angle α from 0° to 70° with $Co_{K\alpha 1}$ radiation in the back reflection mode [22] in a Bruker D8 Discover X-ray diffraction. From the pole figures the orientation distribution function (ODF) was calculated at different thickness layers by the series expansion method ($L_{max}=22$) [23]. The specimens of the as-cast strips and hot rolled strips used for texture measurements were prepared with the size of 22 mm (L) × 20 mm (W). The position along the thickness direction can be defined by a parameter s, as $s=2a/d$, where a and d are the distance away from the center layer and the strip thickness, respectively. The orientation image maps along the longitudinal section (RD–ND) of the hot rolled strips were determined by the electron backscatter diffraction (EBSD) system equipped at a field emission scanning electron microscope (SEM). The tensile tests were conducted at room temperature on a SANS computer controlled universal testing machine. The fracture surfaces were examined by scanning electron microscope (SEM).

3. Results

3.1. Microstructure and texture of the as-cast strips

Figs. 1 and 2 show the microstructure and texture of the fine-grained and coarse-grained as-cast strips, respectively. The microstructure of both as-cast strips consisted of ferrite matrix and martensite. The ferrite matrix in the fine-grained as-cast strip was characterized by outer columnar grains and inner equiaxed grains, as shown in Fig. 1(a). It was measured that the average ferrite grain size was 161 μm. The texture of the fine-grained as-cast strip was characterized by medium {001}⟨0vw⟩ fibre texture in the outer layers $s=0.7$–1.0 and nearly random texture in the inner layers, as shown in Fig. 1(b).

By contrast, the microstructure of the coarse-grained as-cast strip was characterized by large columnar ferrite grains with the average size of 367 μm and martensite, as shown in Fig. 2(a). The texture was mainly characterized by strong {001}⟨0vw⟩ fibre texture through the whole thickness.

3.2. Microstructure and texture of the hot rolled strips

Fig. 3 shows the microstructure of the hot rolled fine-grained and coarse-grained strips. Although the microstructure of all the hot rolled strips was composed of deformed ferrite grains, proeutectoid ferrite grains and pearlite, the hot rolling reduction had a significant influence on the microstructure evolution. The microstructure of both 5% hot rolled strips was quite similar to their initial solidification microstructure, as shown in Fig. 3(a1) and (b1). As the hot rolling reduction increased from 20% to 50%, the

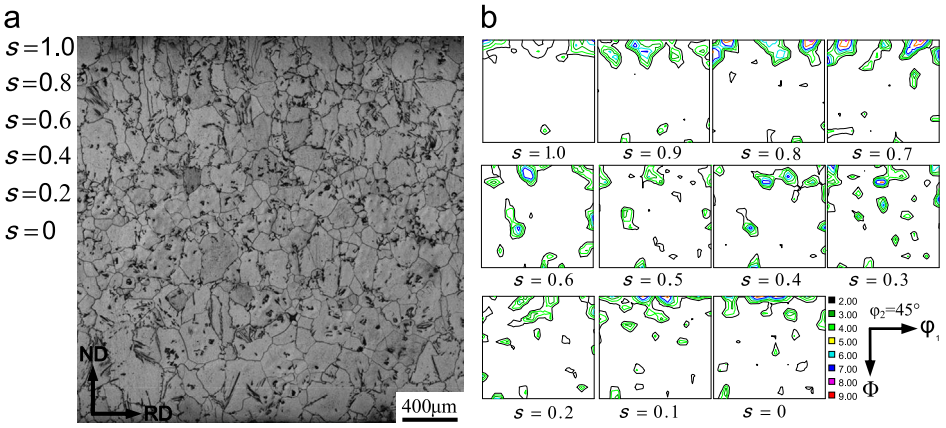

Fig. 1. Microstructure (a) and texture (b) of the fine-grained as-cast strip.

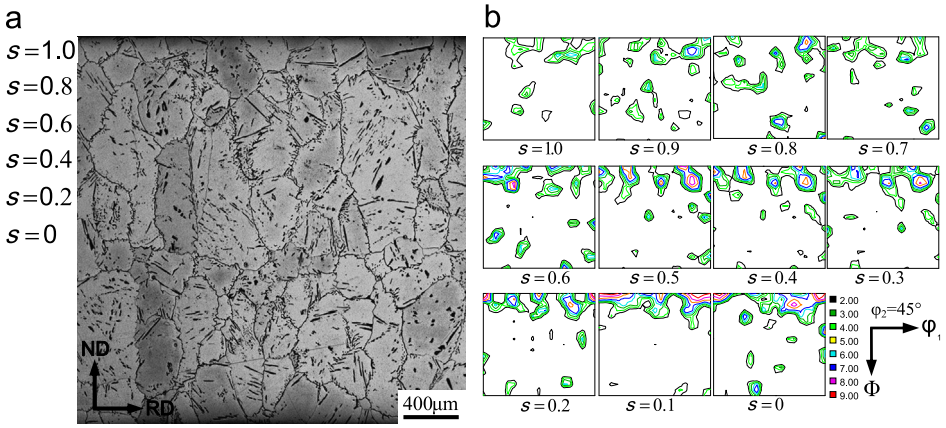

Fig. 2. Microstructure (a) and texture (b) of the coarse-grained as-cast strip.

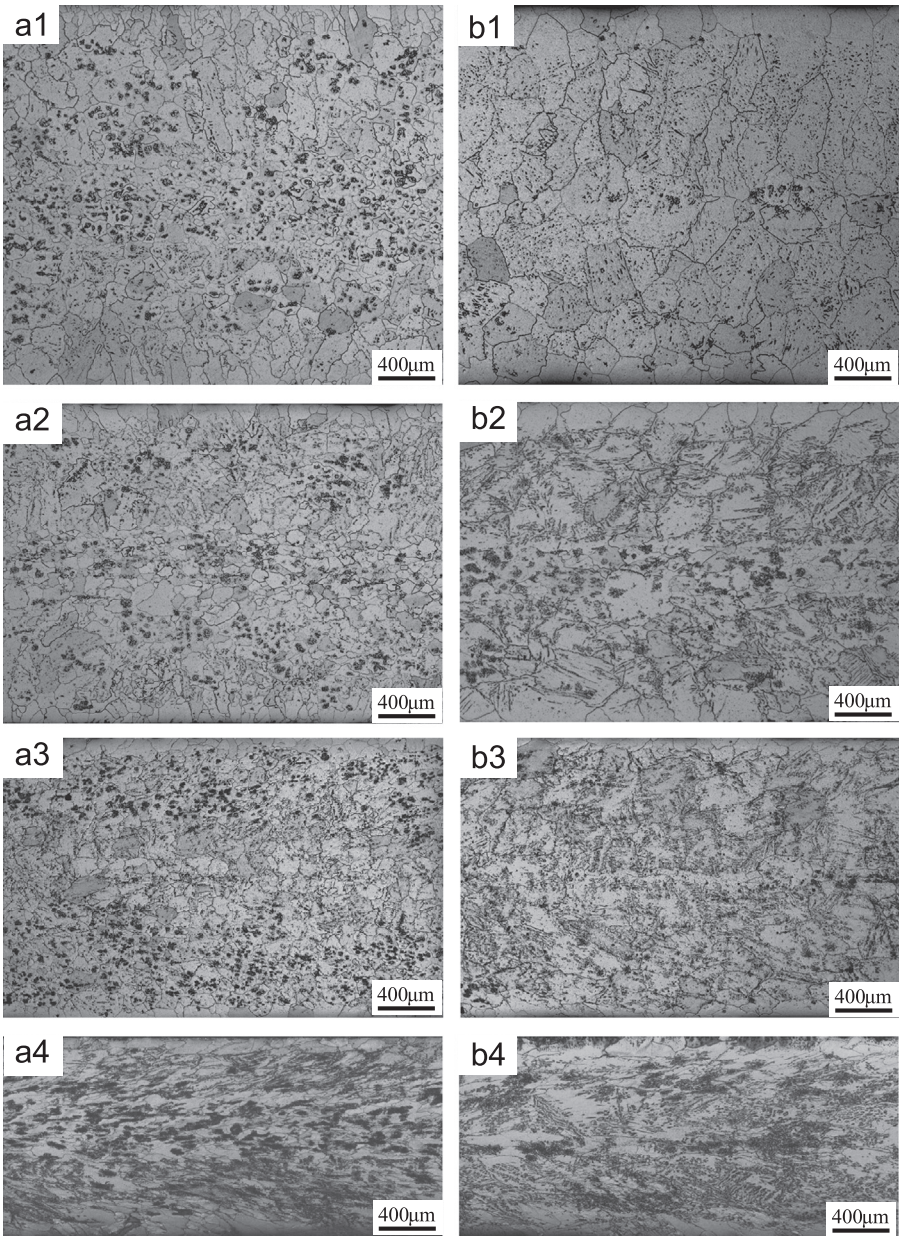

Fig. 3. Effect of hot rolling reduction on the microstructure of the as-cast strips with different initial solidification structures ((a) fine-grained as-cast strip; (b) coarse-grained as-cast strip; 1, 2, 3 and 4 were referred to as 5%, 20%, 30% and 50% reductions, respectively).

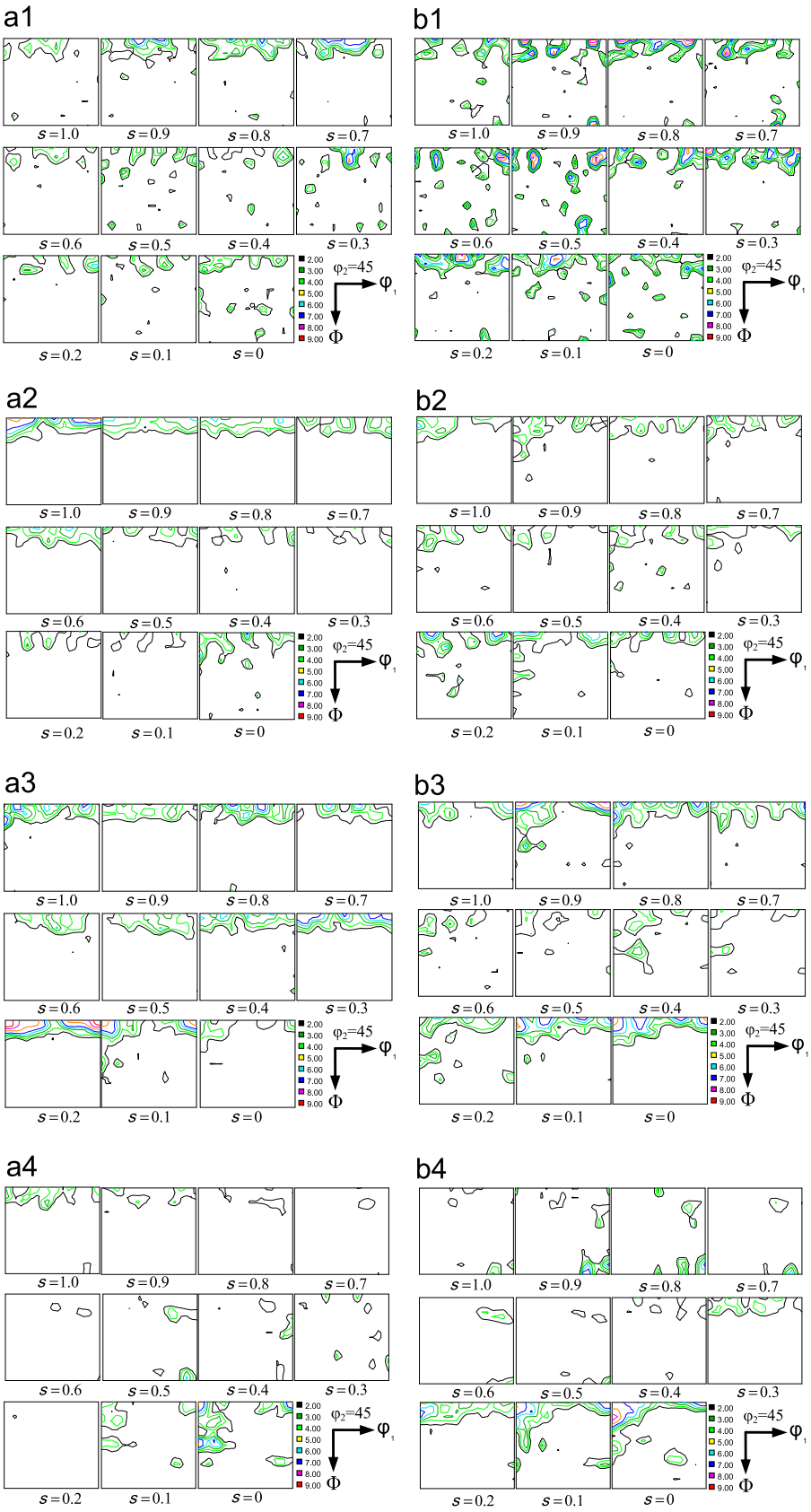

Fig. 4. Effect of hot rolling reduction on the texture of the as-cast strips with different initial solidification structures ((a) fine-grained as-cast strip; (b) coarse-grained as-cast strip; 1, 2, 3 and 4 were referred to as 5%, 20%, 30% and 50% reductions, respectively).

as-cast strips were severely deformed and thus the initial solidification structures were further refined. When the hot rolling reduction was 50%, the deformed ferrite grains were obviously elongated and deviated from the rolling direction due to the severe deformation, as shown in Fig. 3(a4) and (b4). It was found that the hot rolled fine-grained strips showed much finer microstructures than those of the hot rolled coarse-grained strips at the same hot rolling reduction. Besides, the ferrite grain size was more homogeneous in the hot rolled fine-grained strips than that of the hot rolled coarse-grained strips.

Fig. 4 shows the effect of hot rolling reduction on the through-thickness texture of the hot rolled strips. The texture exhibited obvious variations with increasing hot rolling reduction in spite of the different initial solidification structures. The texture of both 5% hot rolled fine-grained and coarse-grained strips was quite similar to their initial solidification texture, as shown in Fig. 4(a1) and (b1). As the hot rolling reduction increased from 20% to 30%, medium {001}⟨0vw⟩ fibre texture evolved throughout the thickness and weak α and γ fibre textures evolved in the center layers of all the hot rolled strips. When the hot rolling was 50%, the texture of both the hot rolled fine-grained and coarse-grained strips was characterized by medium {001}⟨0vw⟩ fibre texture and Goss texture in the surface layers and α and γ fibre textures in the center layers. It was found that the hot rolled coarse-grained strips showed stronger α and γ fibre textures than that of the hot rolled fine-grained strips at the same hot rolling reduction. Besides, strong Goss texture with the maximum intensity of 3.42 times of random distribution evolved in the layers $s=0.5–1.0$ of the 50% hot rolled coarse-grained strip, while relatively weaker Goss texture formed in the layers $s=0.5–0.8$ of the 50% hot rolled fine-grained strips.

3.3. Room temperature ductility of the hot rolled strips

In the present work, the break elongation measured by the tensile tests was used to evaluate the ductility of the hot rolled strips. Fig. 5 shows the effect of hot rolling reduction on the elongations of the hot rolled strips. The elongations were gradually improved with increasing hot rolling reduction in spite of different initial solidification structures. The hot rolled fine-grained strips showed relatively higher elongation than that of the hot rolled coarse-grained strips at the same hot rolling reduction. At the hot rolling reduction of 5–20%, the elongations of the hot rolled fine-grained and coarse-grained strips were almost the same. When the hot rolling reduction was 30–50%, the difference between the elongations of the hot rolled fine-grained and coarse-grained strips was significant. A total reduction of more than 30% was required for the fine-grained strips to achieve relatively good ductility (elongation exceeding 20%), while that for the coarse-grained strips was as high as 50%.

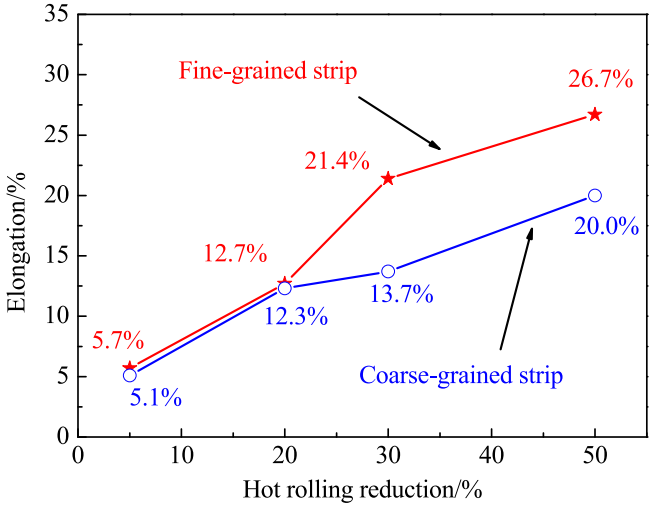

Fig. 5. Effect of hot rolling reduction on the elongation of the hot rolled strips with different initial solidification structures.

Fig. 6 shows the effect of hot rolling reduction on the fracture morphology of the hot rolled strips. The fracture modes of all the hot rolled strips were gradually transformed from brittle fracture to ductile fracture with increasing hot rolling reduction in spite of different initial solidification structures. The fracture surfaces of both 5% hot rolled fine-grained and coarse-grained strips displayed complete cleavage fracture with large cleavage facets, as shown in Fig. 6(a1) and (b1). As the hot rolling reduction increased from 20% to 50%, the amount of ductile fracture bands and dimples increased, which indicated the improvement of the ductility in all the hot rolled strips. The fracture mode of the hot rolled fine-grained strips was transformed into ductile fracture at a total reduction of more than 30%, while that for the coarse-grained strips was as high as 50%. Considering the results shown in Figs. 5 and 6, it should be noted that the variation of the elongation with increasing hot rolling reduction was in good agreement with that of the fracture morphology.

4. Discussion

4.1. Microstructure and texture evolution of the as-cast strips

Liu et al. confirmed that the melt superheat in the pool can affect the temperature gradient in front of the solid phase during strip casting [17,18]. So the melt superheat was the most important factor to determine the solidification structure. When the melt superheat was relatively low, such as 25 °C in this work, the temperature gradient in front of the solid phase could satisfy the selective growth mechanism for some {001} columnar δ-ferrite grains at the early stage of solidification. The columnar ferrite grains in the fine-grained as-cast strip were observed at the surface layers $s=0.7–1.0$ as shown in Fig. 1(a). As columnar δ-ferrite grains grew up, the temperature gradient decreased and the selective growth effect vanished at the end of solidification, thus gave rise to the formation of the equiaxed δ-ferrite grains in the inner layers. By contrast, when the melt superheat was as high as 60 °C, a high temperature gradient could be provided in front of the {001} dendrites tips even at the last stage of solidification and thus led to the well-developed columnar structure, as shown in Fig. 2(a).

During the air-cooling stage after solidification, a certain amount of δ-ferrite transformed into austenite and subsequently transformed into martensite due to the relatively high cooling rate. It is known that the austenite may obey the Kurdjumov–Sachs (K–S) relationship with respect to the parent ferrite during δ→γ transformation [24,25], and the lath martensite obeys the Kurdjumov–Sachs (K–S) or Nishiyama–Wasserman (N–W) orientation relationship with parent austenite during martensite transformation [26,27]. However, in the present work, the volume fraction of martensite in the fine-grained and coarse-grained as-cast strips was only about 3% and 8% respectively due to the very limited δ→γ transformation. Consequently, the transformation type texture was negligible in the as-cast strips and the texture was mainly characterized by the orientations of the initial solidification δ-ferrite. As a result, considering the solidification structure through the thickness (Fig. 1(a)), it could be inferred that the {001}⟨0vw⟩ fibre texture in the outer layers and the nearly random texture in the center layers (Fig. 1(b)) were mainly attributed to the formation of outer columnar δ-ferrite grains and inner equiaxed δ-ferrite

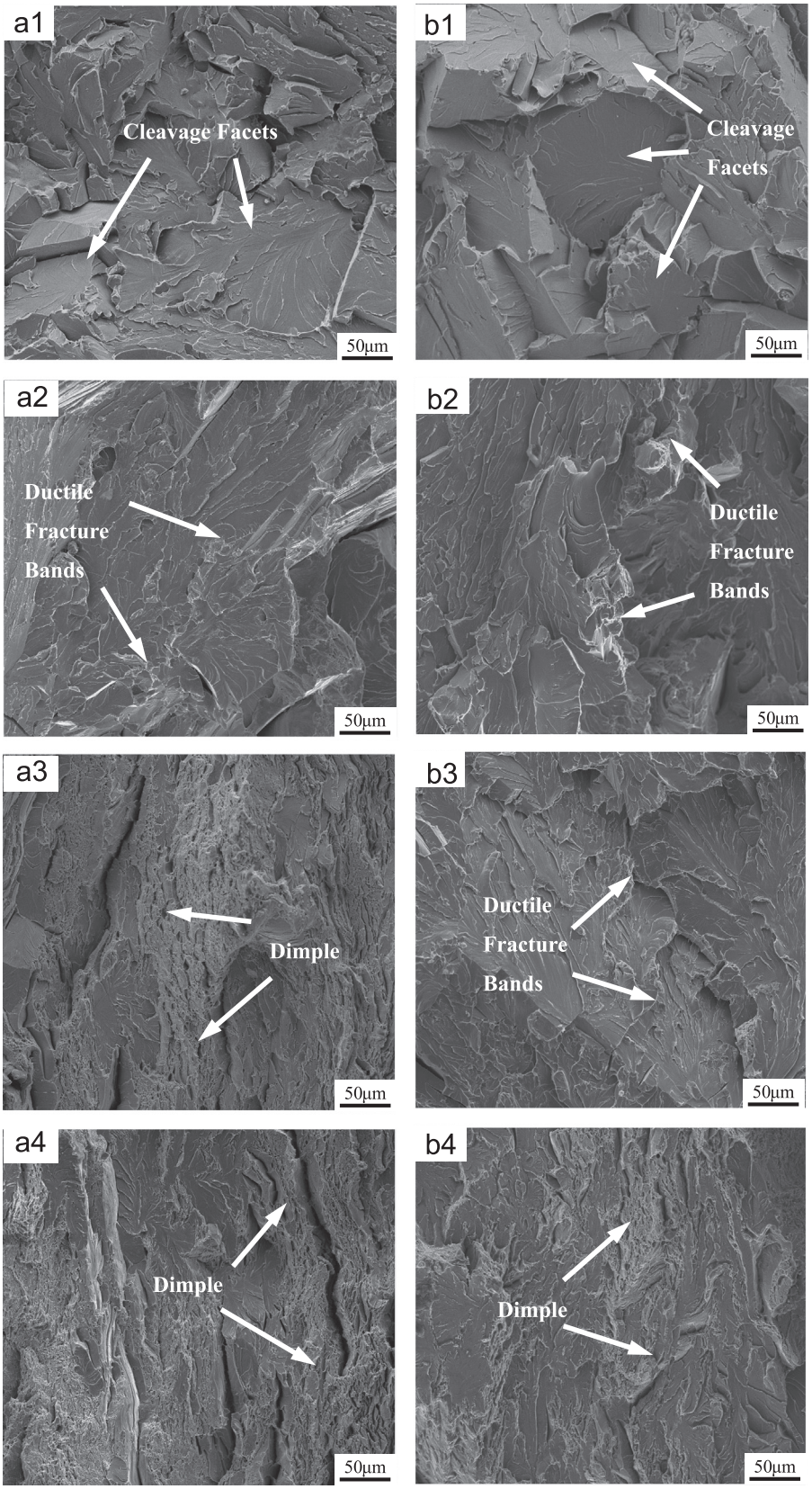

Fig. 6. Effect of hot rolling reduction on the fracture morphology of the hot rolled strips with different initial solidification structures ((a) fine-grained as-cast strip; (b) coarse-grained as-cast strip; 1, 2, 3 and 4 were referred to as 5%, 20%, 30% and 50% reductions, respectively).

grains, respectively. Similarly, the strong {001}⟨0vw⟩ fibre texture through the whole thickness of the coarse-grained as-cast strip (Fig. 2(b)) was attributed to the formation of coarse columnar δ-ferrite grains (Fig. 2(a)).

4.2. Effect of hot rolling reduction on the microstructure evolution

Fig. 7 shows the typical microstructure of the 20% hot rolled coarse-grained strip. According to the calculated phase diagram,

when the as-cast strips were reheated to 1150 °C, the microstructure was composed of about 66.5% (volume fraction) ferrite and 33.5% austenite. During the air-cooling stage after hot rolling, partial austenite was transformed into proeutectoid ferrite when the temperature was below A_3 temperature and subsequently the rest of austenite was transformed into pearlite when the temperature was below A_1 temperature.

Fig. 8 shows the grain boundary misorientation distribution of the 20% hot rolled strips. The large ferrite grains were surrounded by high-angle boundaries, while extensive low-angle boundaries were observed inside these grains. It is known that the ferrite in silicon steel has high stacking fault energy and it mainly undergoes dynamic recovery during hot rolling [28,29]. As a result, the large elongated ferrite grains were formed by rapid dynamic recovery. It was observed that the small ferrite grains formed in the large ferrite grains were surrounded by high-angle boundaries, free of low-angle boundaries and co-existed with the pearlite, as shown in Fig. 7. Thus, it could be inferred that the small ferrite grains were not recrystallized grains but proeutectoid ferrite grains by γ→α+P transformation during the cooling stage after hot rolling.

The average ferrite grain size of the fine-grained as-cast strip was 161 μm, while that of the coarse-grained as-cast strip was as large as 367 μm. As a result, the microstructure of the hot rolled fine-grained strips was much finer at the same hot rolling reduction due to the relatively finer initial solidification structure. It is known that the fine-grained steels exhibited superior compatible deformation capability due to the small differences between the deformation in the vicinity of the boundaries and the interior of the grains [30,31]. Consequently, the deformation in the grains of fine-grained strips was more uniform, thus gave rise to more homogeneous microstructure, as shown in Fig. 3.

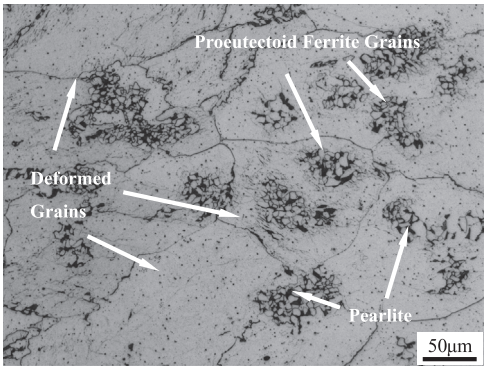

Fig. 7. High magnification microstructure of the 20% hot rolled coarse-grained strip.

4.3. Effect of hot rolling reduction on the texture evolution

The texture of the hot rolled strips was mainly characterized by the orientations of the deformed ferrite grains due to the limited γ→α+P transformation. Figs. 9–11 show the effect of hot rolling reduction on λ, α and γ fibre textures in the center layer of the hot rolled strips with different initial solidification structures, correspondingly. It was found that both 20% hot rolled fine-grained and coarse-grained strips showed the strongest {001}⟨100⟩ component and very weak α and γ fibre textures. As the hot rolling reduction increased from 20% to 50%, the intensity of {001}⟨100⟩ component decreased, while those of α and γ fibre textures greatly increased. It is known that the plane strain dominates in the center layer of the sheet and the plane strain increases with increasing hot rolling reduction [7]. Consequently, the plane strain compression textures (α and γ fibre textures) [3] were gradually enhanced at the expense of the initial solidification texture ({001}⟨100⟩ component) in the center layer, as shown in Figs. 9–11, and the intensity variation of λ, α and γ fibre textures was in good agreement with increasing hot rolling reduction. The hot rolled coarse-grained strips exhibited relatively stronger λ, α and γ fibre textures at the same hot rolling reduction, which was mainly related with the initial stronger solidification texture, as shown in Fig. 4.

Fig. 12 shows the through-thickness variation of Goss texture intensity in hot rolled strips. It was found that, when the hot rolling reduction was 5–30%, Goss texture was very weak. At the hot rolling reduction of 50%, Goss texture was greatly enhanced in both hot rolled strips, though relatively stronger Goss texture was observed in the hot rolled coarse-grained strip. It is known that Goss texture is formed by shear deformation under high frictional force between the roll and hot rolled sheet surface [32], and the shear deformation increases with rolling reduction [33–35]. When the hot rolling reduction was 5–30%, the shear deformation was

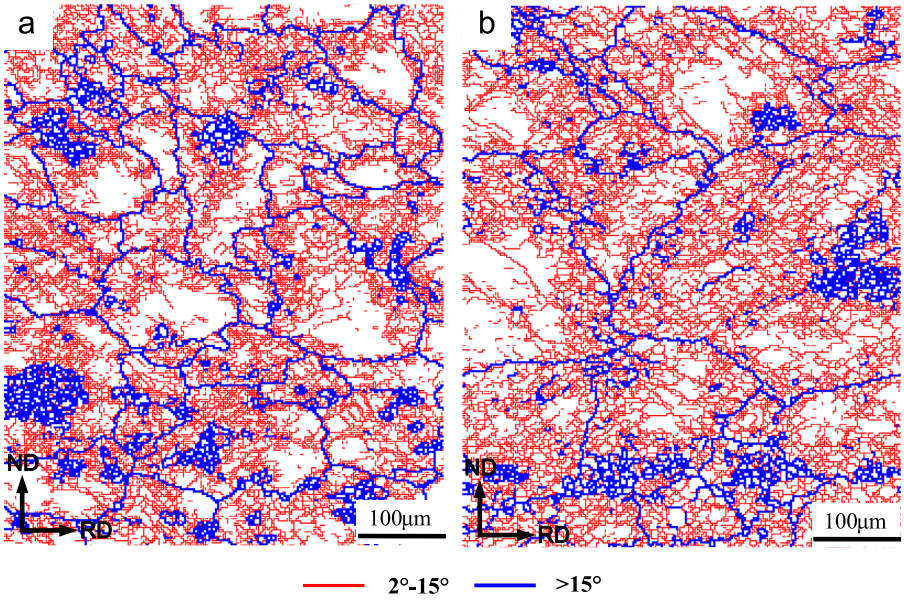

Fig. 8. Grain boundary misorientation distribution of the 20% hot rolled strip with initial (a) fine-grained and (b) coarse-grained solidification structures.

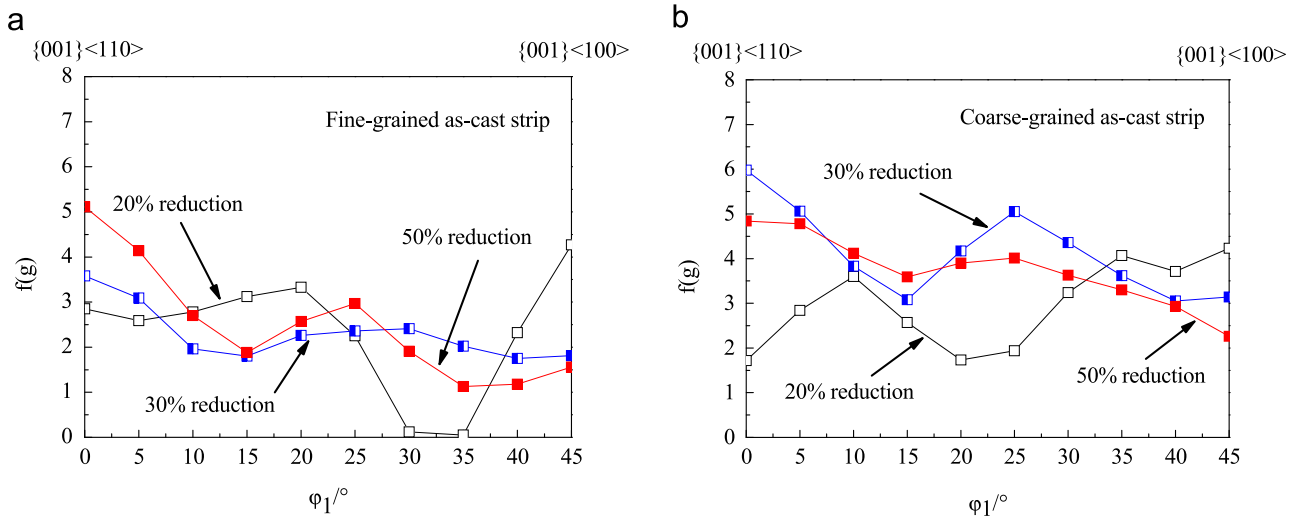

Fig. 9. Effect of hot rolling reduction on orientation intensities along λ fibre in the center layer of the hot rolled strips with initial (a) fine-grained and (b) coarse-grained solidification structures.

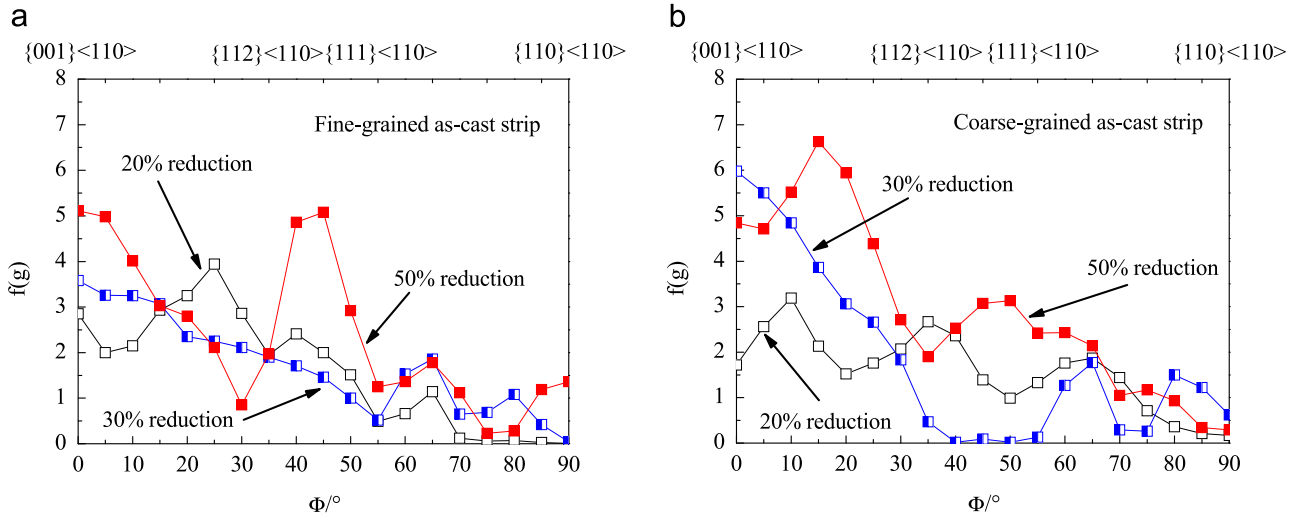

Fig. 10. Effect of hot rolling reduction on orientation intensities along α fibre in the center layer of the hot rolled strips with initial (a) fine-grained and (b) coarse-grained solidification structures.

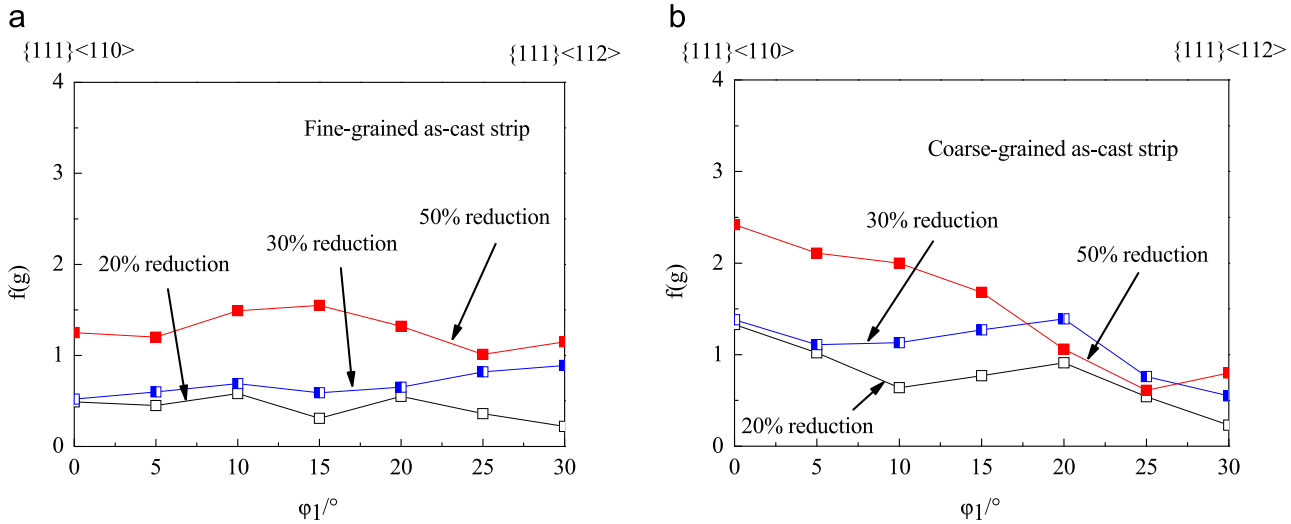

Fig. 11. Effect of hot rolling reduction on orientation intensities along γ fibre in the center layer of the hot rolled strips with initial (a) fine-grained and (b) coarse-grained solidification structure.

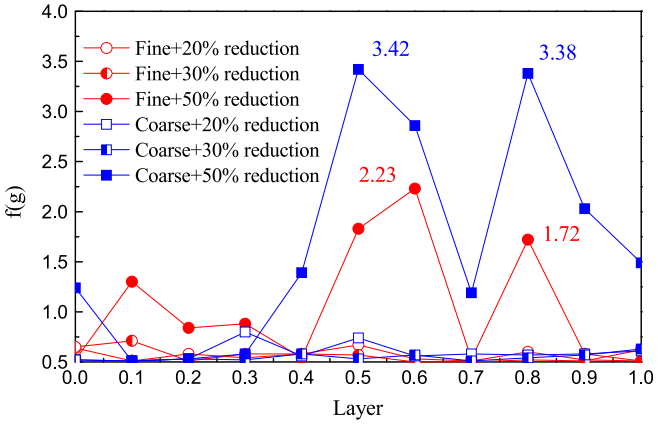

Fig. 12. Effect of hot rolling reduction on the intensity of Goss texture in the hot rolled strips with different initial solidification structures (fine–fine grained structure, coarse–coarse grained structure).

quite weak, thus gave rise to very weak Goss texture. At the hot rolling reduction of 50%, severe shear deformation evolved in the strips and led to strong Goss texture. It is known that the coarse-grained as-cast strip exhibits relatively inferior compatible deformation capability. It means that the plastic strain between neighboring grains may not be readily accommodated by homogeneous deformation and, thus, nonhomogeneous deformation (shear deformation) may be triggered to achieve the macro-strain compatibility. Consequently, much severe shear deformation may evolve in the hot rolled coarse-grained strip and, thus, leads to stronger Goss texture, as shown in Fig. 12. Fig. 13 shows the orientation image map and Goss orientation of the 50% hot rolled strips. Strong Goss texture evolved in the large deformed ferrite grains in the layers $s=0.5$–1.0 of the hot rolled coarse-grained strip, while relatively weak Goss texture formed in the hot rolled fine-grained strip. Interesting to note that the Goss texture in both 50% hot rolled strips showed a few obvious peaks, as shown in Fig. 12. This may be mainly related with the especial rolling

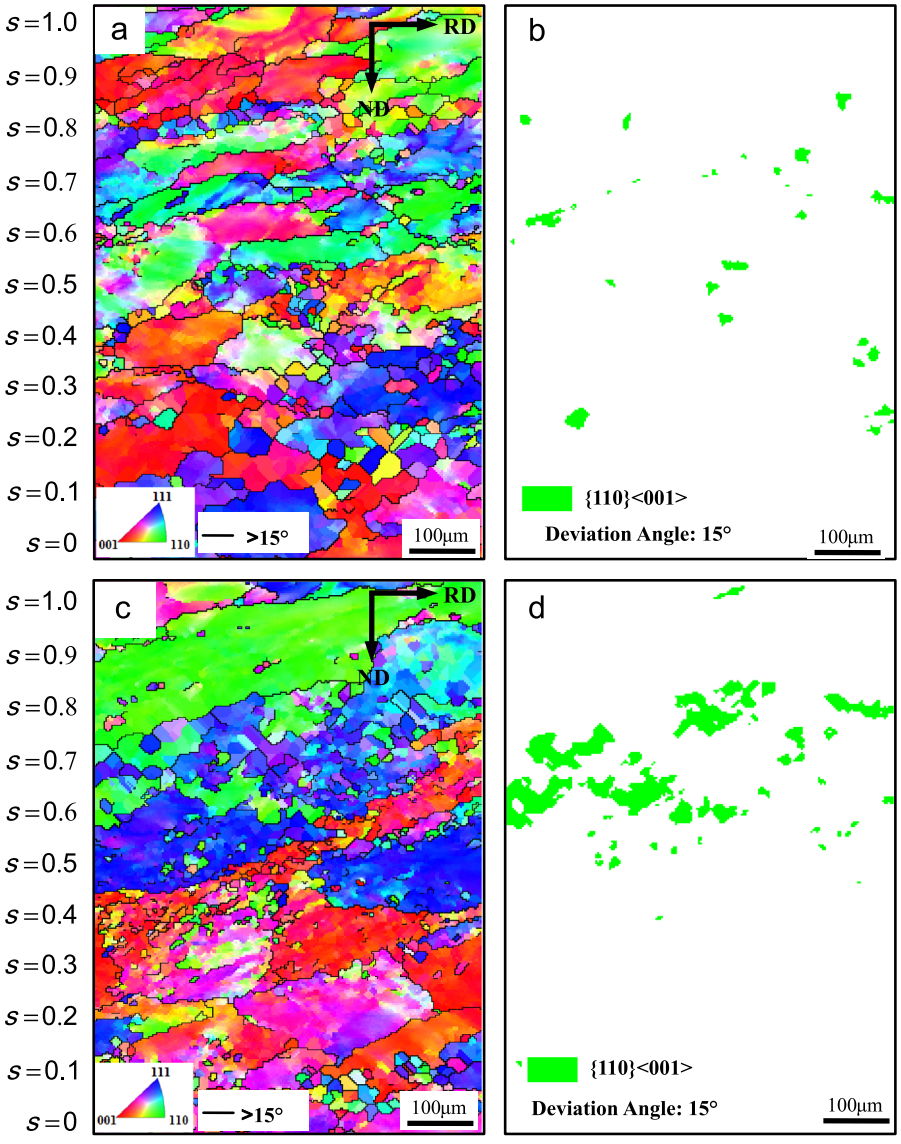

Fig. 13. Orientation image maps of all orientations (a) and Goss orientation (b) of the 50% hot rolled fine-grained strip and orientation image map of all orientations (c) and Goss orientation (d) of the 50% hot rolled coarse-grained strip.

process, i.e. two passes, which led to a shear deformation distribution through thickness unlike single-pass hot rolling. However, more attention should be paid to this interesting phenomenon.

4.4. Effect of hot rolling reduction on the room temperature ductility

It is known that the ductility of the steel within the traditional grain size regime can be improved by refining grains due to the improvement of the compatible deformation capability [36]. In the present work, the microstructures of the hot rolled strips were gradually refined and became more homogeneous with increasing hot rolling reduction. Thus, the elongations were gradually improved, as shown in Fig. 5. And, it was observed that the number of ductile dimples and ductile fracture bands increased, which indicated the gradual improvement of the ductility. However, the hot rolled fine-grained strips exhibited relatively finer microstructures at the same reduction due to finer initial solidification structures. Consequently, hot rolled fine-grained strips exhibited relatively higher elongations (better ductility).

In addition, the texture evolution may also have an effect on the ductility of the tested steel. It is known that the ductility may increase considerably since the grains in a favorable orientation suited to accommodate the imposed strain [37]. In the present work, the texture exhibited obvious evolution with the increasing hot rolling reduction. However, this influence is still not very clear now. This should be paid more attention in the future work.

5. Conclusions

In this study, the grain-oriented silicon steel as-cast strips with different initial solidification structures were produced by strip casting and followed by hot rolling with various reductions. The effects of hot rolling reduction on the microstructure, texture and ductility were investigated. In summary, the conclusions are summarized as follows:

(1) The fine-grained and coarse-grained as-cast strips can be produced at relatively low and high melt superheat, respectively. Although the microstructure was composed of ferrite matrix and martensite in both as-cast strips, the textures were significantly different due to the dissimilar solidification conditions during strip casting.
(2) The microstructure of all the hot rolled strips was composed of deformed ferrite grains, proeutectoid ferrite grains and pearlite, and it was refined with increasing hot rolling reduction. Thus, the elongation was gradually improved and the fracture mode was transformed from brittle fracture to ductile fracture with increasing hot rolling reduction. The hot rolled fine-grained strips showed much finer microstructure at the same hot rolling reduction, thus gave rise to the superior ductility. A total reduction of more than 30% was required for the fine-grained strips to achieve relatively good ductility, while that for the coarse-grained strips was as high as 50%.
(3) With increasing hot rolling reduction, α and γ fibre textures were enhanced at the expense of the initial solidification texture. At the hot rolling reduction of 5–30%, Goss texture was very weak in the hot rolled strips, but significantly enhanced at the hot rolling reduction of 50%. The 50% hot rolled coarse-grained strip showed much stronger Goss texture than the 50% hot rolled fine-grained strip.

Acknowledgments

This work was supported by the National Natural Science Foundation of China (Grant nos. 50734001, 51004035, 51374002, 51074051, U1260204), the National Key Technology R&D Program (Grant no. 2012BAE03B00), the National High Technology R&D "863" Program (Grant no. 2012AA03A506) and the Fundamental Research Funds for the Central Universities (Grant no. N120407009).

References

[1] V. Stoyka, F. Kováč, O. Stupakov, I. Petryshynets, Mater. Charact. 61 (2010) 1066–1073.
[2] T. Kubota, M. Fujikura, Y. Ushigami, J. Magn. Magn. Mater. 215–216 (2000) 69–73.
[3] S. Mishra, C. Darmann, K. Lucke, Acta Metall. 32 (1984) 2185–2201.
[4] N.P. Goss, U. S. Patent 1965559, 1934.
[5] D. Senk, Ch. Schneider, R. Kopp, Steel Times Int. 14 (1991) 46.
[6] H. Litterscheidt, R. Hammer, C. Schneider, R.W. Simon, D. Senk, R. Kopp, et al., Stahl Eisen. 111 (1991) 61–66.
[7] J.Y. Park, K.H. Oh, H.Y. Ra, ISIJ Int. 40 (2000) 1210–1215.
[8] A.R. Buchner, J.W. Schmitz, Steel Res. 63 (1992) 7–11.
[9] J.C. Grosjean, J.L. Jacquot, J.M. Damasse, H. Literscheidt, D. Senk, W. Schmitz, Iron Mak. Steel Mak. 20 (1993) 27–32.
[10] D. Raabe, Acta Metall. Mater. 45 (1997) 1137–1151.
[11] J.Y. Park, K.H. Oh, H.Y. Ra, Scr. Mater. 40 (1999) 881–885.
[12] W. Truszkowski, J. Krol, B. Major, Metall. Trans. 11A (1980) 749–758.
[13] W. Truszkowski, J. Krol, B. Major, Metall. Trans. 13A (1982) 665–669.
[14] Y. Shimizu, Y. Ito, Y. Iida, Metall. Trans. A 17A (1986) 1323–1334.
[15] M. Matsuo, ISIJ Int. 29 (1989) 809–827.
[16] E.E.M. Luiten, K. Blok, Energy Policy 31 (2003) 1339–1356.
[17] H.T. Liu, Z.Y. Liu, Y.Q. Qiu, G.M. Cao, C.G. Li, G.D. Wang, Mater. Charact. 60 (2009) 79–82.
[18] H. Liu, Z. Liu, C. Li, G. Cao, G. Wang, Mater. Charact. 62 (2011) 463–468.
[19] H. Liu, Z. Liu, G. Cao, C. Li, G. Wang, J. Magn. Magn. Mater. 323 (2011) 2648–2651.
[20] H.T. Liu, Z.Y. Liu, Y. Sun, Y.Q. Qiu, C.G. Li, G.M. Cao, B.D. Hong, S.H. Kim, G.D. Wang, Mater. Lett. 81 (2012) 65–68.
[21] H.T. Liu, Z.Y. Liu, Y.Q. Qiu, Y. Sun, G.D. Wang, J. Mater. Process. Technol. 212 (2012) 1941–1945.
[22] L.G. Schulz, J. Appl. Phys. 20 (1949) 1030–1033.
[23] H.J. Bunge, Z. Metallkd. 56 (1965) 872–874.
[24] K. Ameyama, G.C. Weatherly, K.T. Aust, Acta Metall. Mater. 8 (1992) 1835–1846.
[25] C.H. Shek, C. Dong, J.K.L. Lai, K.W. Wong, Metall. Trans. A 31A (2000) 15–19.
[26] S. Morito, H. Tanaka, R. Konishi, T. Furuhara, T. Maki, Acta Mater. 51 (2003) 1789–1799.
[27] G. Miyamoto, N. Iwata, N. Takayama, T. Furuhara, Acta Mater. 58 (2010) 6393–6403.
[28] H.J. McQueen, Metall. Trans. A 8A (1977) 807–824.
[29] J.L. Walter, E.F. Koch, Trans. Metall. Soc., AIME 233 (1965) 1209–1220.
[30] R. Abbaschian, L. Abbaschian, R.E. Reed-Hill, Physical Metallurgy Principles, Cengage Learning, Stamford, 2009.
[31] B. Bay, N. Hansen, D.A. Hughes, D. Kuhlmann-Wilsdorf, Acta Metall. Mater. 40 (1992) 205–219.
[32] P. Rodriguez-Calvillo, Y. Houbaert, R. Petrov, L. Kestens, R. Colas, Mater. Chem. Phys. 136 (2012) 710–719.
[33] S. Matsumura, Y. Tanaka, Y. Koga, K. Oki, Mater. Sci. Eng. A A312 (2001) 284–292.
[34] D. Raabe, M. Ylitalo, Metall. Mater. Trans. A 27A (1996) 49–57.
[35] D. Raabe, Steel Res. 74 (2003) 327–337.
[36] M.A. Meyers, S. Mishra, D.J. Benson, Prog. Mater. Sci. 51 (2006) 427.
[37] Qinghuan Huo, Xuyue Yang, Huan Sun, Bin Li, Jia Qin, Jun Wang, Jijun Ma, J. Alloys Compd. 581 (2013) 230–235.